# Low-spin states in $^{80}$ Ge populated in the $\beta$ decay of the $^{80}$ Ga 3<sup>-</sup> isomer

S. Sekal, <sup>1,2,\*</sup> L. M. Fraile, <sup>3,†</sup> R. Lică, <sup>2,4</sup> M. J. G. Borge, <sup>5</sup> W. B. Walters, <sup>6</sup> A. Aprahamian, <sup>7</sup> C. Benchouk, <sup>1</sup> C. Bernards, <sup>8,9</sup> J. A. Briz, <sup>5</sup> B. Bucher, <sup>10</sup> C. J. Chiara, <sup>6,11,‡</sup> Z. Dlouhý, <sup>12,§</sup> I. Gheorghe, <sup>4</sup> D. G. Ghiţă, <sup>4</sup> P. Hoff, <sup>13</sup> J. Jolie, <sup>8</sup> U. Köster, <sup>14</sup> W. Kurcewicz, <sup>15</sup> H. Mach, <sup>3,16,§</sup> N. Mărginean, <sup>4</sup> R. Mărginean, <sup>4</sup> Z. Meliani, <sup>1</sup> B. Olaizola, <sup>2,3</sup> V. Paziy, <sup>3</sup> J. M. Régis, <sup>8</sup> M. Rudigier, <sup>8</sup> T. Sava, <sup>4</sup> G. S. Simpson, <sup>17,18</sup> M. Stănoiu, <sup>4</sup> and L. Stroe<sup>4</sup> <sup>1</sup>Laboratoire Sciences Nucléaires et Interactions Rayonnements-Matière, USTHB, BP 32 El-Alia, 16011 Bab Ezzouar Alger, Algérie <sup>2</sup>CERN, CH-1211 Geneva 23, Switzerland <sup>3</sup> Grupo de Física Nuclear & IPARCOS, Facultad de Ciencias Físicas, Universidad Complutense de Madrid - CEI Moncloa, 28040 Madrid, Spain <sup>4</sup> "Horia Hulubei" National Institute of Physics and Nuclear Engineering, 077125 Bucharest, Romania <sup>5</sup>Instituto de Estructura de la Materia, CSIC, 28006 Madrid, Spain <sup>6</sup>Department of Chemistry and Biochemistry, University of Maryland, College Park, Maryland 20742, USA <sup>7</sup>Department of Physics, University of Notre Dame, Notre Dame, Indiana 46556, USA <sup>8</sup>Institut für Kernphysik, Universität zu Köln, Zülpicher Strasse 77, 50937 Köln, Germany <sup>9</sup>Wright Nuclear Structure Laboratory, Yale University, New Haven, Connecticut 06520, USA <sup>10</sup>Idaho National Laboratory, Idaho Falls, Idaho 83415, USA <sup>11</sup>Physics Division, Argonne National Laboratory, Argonne, Illinois 60439, USA <sup>12</sup>Nuclear Physics Institute of the Czech Academy of Sciences, 25068, Řež, Czech Republic <sup>13</sup>Department of Chemistry, University of Oslo, 0316 Oslo, Norway <sup>14</sup>Institut Laue-Langevin, 38042 Grenoble, France <sup>15</sup>Faculty of Physics, University of Warsaw, Pasteura 5, 02-093 Warsaw, Poland <sup>16</sup>National Centre for Nuclear Research, BP1, ul. Hoża 69, 00-681, Warsaw, Poland <sup>17</sup>LPSC-IN2P3, Université Grenoble Alpes, CNRS, Grenoble INP, 38000 Grenoble, France



(Received 20 October 2020; revised 23 July 2021; accepted 27 July 2021; published 10 August 2021)

<sup>18</sup>School of Engineering, University of the West of Scotland, Paisley PA1 2BE, United Kingdom

The structure of  $^{80}$ Ge has been investigated at the ISOLDE facility at CERN. A previous study reported for the first time a low-lying  $0_2^+$  intruder state at 639 keV, based on the coincidence with a previously unobserved 1764-keV  $\gamma$  ray, and suggested it as evidence for shape coexistence in  $^{80}$ Ge. We used the  $\beta$  decay from the 3<sup>-</sup> 22.4-keV state in  $^{80}$ Ga to enhance the population of low-spin states in  $^{80}$ Ge, including any excited  $0^+$  level, and  $\gamma\gamma$  coincidences to investigate it. We observed a 1764-keV  $\gamma$  ray in coincidence with strong transitions in  $^{80}$ Ge, thus not feeding the proposed 639-keV  $0_2^+$ . No connecting transitions from previously known levels to the 639-keV and 2403-keV  $2_3^+$  states could be established either. Shell-model calculations for Ge isotopes and N=48 isotones were performed. They succeed to explain most of the experimental levels, but fail to reproduce the presence of a  $0_2^+$  state below  $\approx$ 1200 keV in  $^{80}$ Ge. Our experimental findings and shell-model calculations are difficult to reconcile with a very low-lying  $0_2^+$  state in  $^{80}$ Ge.

DOI: 10.1103/PhysRevC.104.024317

## I. INTRODUCTION

The evolution of shell structure in neutron-rich nuclei is a topic of strong interest in modern nuclear structure

Published by the American Physical Society under the terms of the Creative Commons Attribution 4.0 International license. Further distribution of this work must maintain attribution to the author(s) and the published article's title, journal citation, and DOI.

studies. The competition and coexistence at low energy of the configurations arising from the standard shell-model orbitals and those originating from excitations across shell gaps have been identified in several areas of the table of nuclei. The latter (intruder) configurations may exhibit different collective properties than the normal ones, which could be interpreted as a distinct intrinsic shape once an appropriate reference frame is defined.

In the even-even nuclei, the presence of  $0^+$  low-lying excited states above the  $0^+$  ground state (g.s.) may be a signature of shape coexistence. The discovery of the first-excited  $0^+$  state in the doubly-magic  $^{16}$ O, and its interpretation as arising from excitations of several nucleons across the shell closure [1,2], with the additional property of deformation, is probably the first description of this phenomenon in atomic nuclei.

<sup>\*</sup>sekal.ism@hotmail.com

<sup>†</sup>lmfraile@ucm.es

<sup>&</sup>lt;sup>‡</sup>Present address: U.S. Army Research Laboratory, Adelphi, Maryland 20783, USA.

<sup>§</sup>Deceased.

Shape coexistence was suggested also for the doubly-closed N = Z isotope <sup>40</sup>Ca [3]. A microscopic shell-model approach was invoked to explain the onset of deformation, due to protons and neutrons filling orbitals with good overlap in the proximity of closed (sub)shells [4].

With the experimental study of exotic nuclei far from stability in the 1980s, the disappearance of some magic numbers and the appearance of new ones was highlighted and interpreted as the existence of an island of inversion for the N=20 region around  $^{32}$ Mg [5]. For high neutron to proton ratios, the N=20 gap can no longer prevent excitations, and the correlations lead to shape coexistence, where intruder states become more bound than normal states. The phenomenon exists in other regions of the nuclear chart [6], and it appears as a first excited low-lying state  $0^+$  in even-even nuclei, which results from the mixing of configurations with different shapes or from the shift of a pair of nucleons across a subshell.

In the region of intermediate masses, the  $^{78}$ Ni is expected to be a doubly-magic nucleus due to the robust Z=28 and N=50 shell gaps arising from the spin-orbit splitting. The proton to neutron ratio is substantially high and nuclei near  $^{78}$ Ni are particularly exotic, which makes them difficult to reach and investigate experimentally [7]. The evidence for the doubly-magic nature of  $^{78}$ Ni has been recently obtained by Taniuchi *et al.* [8]. Nevertheless, the role of collective effects, with the appearance of deformed states at low excitation, has also been pointed out [8]. This is one of the reasons for the interest of this exotic area of the nuclear chart and why the coexistence of nuclear shapes at low excitation energies may provide information on the forces that drive nuclear structure changes in exotic nuclei.

The neutron-rich Z=32 Ge isotopes with  $32 \leqslant N \leqslant 50$  are important in this context. They are characterized by four protons in the pf shell outside of the Z=28 closed shell, with collective quadrupole excitations dominated by the excitation of valence particles outside of closed shells. These relatively simple nuclear systems with few valence particles can be treated rather precisely within the shell model. They may reveal simple excitation modes that illustrate the competition of single-particle and quadrupole collective motion. For heavier Ge isotopes the investigation of the magicity of the N=50 neutron number far from stability has revealed the persistence of this gap towards Ni (Z=28) with an observed minimum at Z=32 which can be associated with a maximum of collectivity [7].

In this paper we address the population of the reported  $0_2^+$  state [9] in  $^{80}$ Ge (Z=32,N=48) and identify other low-spin states by means of  $\gamma$  spectroscopy. We take advantage of the expected enhanced feeding of these states compared to previous works, thanks to the  $^{80}$ Ge population in the  $\beta$  decay chain of laser-ionized  $^{80}$ Zn. The  $^{80}$ Zn  $0^+$  ground state mostly decays to the  $^{80}$ Ga  $3^-$  isomer [10], which then  $\beta$  decays to  $^{80}$ Ge. Shell-model calculations have been performed to address the location and population of the first-excited  $0_2^+$  state.

#### II. PHYSICS CASE

The study of the structure of N = 48 isotones is of strong interest, as their levels contain combinations of both proton

and neutron excitations. They complement studies of N = 50isotones where only proton excitations involving the  $f_{5/2}$ ,  $p_{3/2}$ , and  $p_{1/2}$  proton levels are found at low energy. One important difference between these nuclei and the N = 50isotones is the possibility to form an 8<sup>+</sup> level with an aligned broken pair of  $g_{9/2}$  neutrons. Some of these states for a number of N = 48 isotones have been reported by Makishima et al. [11]. Another significant difference is the presence of negative-parity levels at low energy in the N=48 isotones, also absent in the N = 50 isotones. These include states in which a deeper  $p_{1/2}$  or  $f_{5/2}$  neutron pair is broken and promoted into the empty  $g_{9/2}$  neutron orbital to produce both a 4<sup>-</sup> and 5<sup>-</sup> doublet, as well as six levels with spins from 2<sup>-</sup> to  $7^-$ . The positions of these levels as well as that of the  $8^+$ state mentioned above are a measure of the energy required to break a neutron pair.

For the  $^{72-78}$ Ge Z=32 even-even isotopes collectivity can be achieved thanks to the additional valence nucleons. The structural changes along the Ge isotopic chain above N=40 are rather intriguing, especially due to the existence of lowlying excited  $0^+$  states [12]. In the case of the  $^{72}$ Ge with N=40, the  $0^+_2$  is the first-excited state, located below the first  $2^+$  level, the latter being interpreted as a member of a rotational band built on the low-lying  $0^+$  state [13]. While a spherical shape for the  $0^+_2$  state in  $^{72}$ Ge is proposed in [14], Ayangeakaa *et al.* [15] suggested triaxially deformed configurations for both the  $0^+_1$  and  $0^+_2$  states. The excitation energy of the second  $0^+$  is much higher in other Ge isotopes, both above and below N=40, and including the N=50 nucleus  $^{82}$ Ge. The systematics of the  $0^+_2$  states are presented and thoroughly discussed in Sec. V.

In this paper we focus on <sup>80</sup>Ge. The properties of its lowlying states have been studied using different methods. The first identification came from the  $\beta$ -n decay of <sup>81</sup>Ga and  $\beta$  decay of <sup>80</sup>Ga [16]. The authors suggested the possibility of two  $\beta$ -decaying states in  $^{80}$ Ga based on the quasidegeneracy of the  $p_{1/2}$  and  $g_{9/2}$  configurations, but were not able to distinguish them. The existence of two  $\beta$ -decaying states was confirmed by colinear laser spectroscopy [17], where a long-lived lowlying isomeric state was found. A more recent study [18,19] attempted to assign  $\gamma$  rays to the decay of the two isomers, with 1.9(1) and 1.3(2) s half-lives, on the basis of the time dependence of the  $\gamma$ -ray spectra from the decay of  $^{80}$ Ga source with an admixture of both isomers. These  $\beta$ -decay studies have suffered from the ambiguity of the  $\beta$ -decaying states in 80Ga, which has been recently clarified as a 6- ground state and a  $3^ \beta$ -decaying isomer at only 22.4 keV [10]. The studies mentioned above provide a consistent picture of the <sup>80</sup>Ge structure populated in  $\beta$  decay.

Other experiments have used Coulomb excitation in inverse kinematics [20] and deep-inelastic scattering reactions. A  $^{82}$ Se beam on  $^{198}$ Pt [11] and  $^{192}$ Os [21] targets was used to populate the ground-state band up to the  $8^+$  state, with a proposed neutron two-hole  $g_{9/2}$  configuration for the yrast states. Lifetime measurements were performed by Mach *et al.* [22], who reported a  $T_{1/2} = 2.95(6)$  ns value for the  $8^+ \rightarrow 6^+$  transition. Other deep-inelastic studies include the work by Faul *et al.* [23], who tentatively extended the yrast band to the  $10^+$  state and identified many previously unobserved

transitions. The latter is confirmed by the recent work by Forney *et al.* [24] using multinucleon transfer reactions on uranium targets. All these studies are very well in agreement with the observations in  $\beta$  decay. All in all, a coherent picture of the excited structure of <sup>80</sup>Ge is believed to exist.

Nonetheless, Gottardo *et al.* [9] surprisingly reported a low-lying 639(1)-keV  $0_2^+$  state in  $^{80}$ Ge, below the previously measured  $2^+$  state, and interpreted it as a two-neutron excitation across N=50. The nucleus  $^{80}$ Ge was populated in the  $\beta$  decay of an  $^{80}$ Ga isomer mix at the ALTO facility, where  $\gamma$  and conversion electron spectroscopy was performed. As a  $0_2^+$  state could not be directly populated from a  $3^-\beta$ -decaying parent, a new weak  $\gamma$  transition at 1764(1) keV that had not been reported in [16] was proposed as a transition from a newly established 2403(1)-keV  $2^+$  level that could populate it. The placement of the  $0_2^+$  state in  $^{80}$ Ge at 639 keV was based on the observation of a new electron conversion line at 628(1) keV in coincidence with the 1764(1)-keV  $\gamma$  ray.

Very recently García *et al.* [25] conducted a similar experiment with enhanced statistics using a mixed  $^{80}$ Ga source as well. No evidence was found in the conversion-electron spectroscopy for the 639-keV  $0_2^+$  to  $0_1^+$  transition. Moreover, several peaks in the 1764-keV energy region were identified in the coincidence gates set on the  $\gamma$  rays that depopulate the  $5^-$ ,  $6^+$ , and  $8^+$  levels.

All the previous  $\beta$ -decay studies have the common feature of the use of  $^{80}$ Ga decay sources with mixed  $3^-$  and  $6^-$  states. The source used for the data reported in the present work is obtained by growing  $^{80}$ Ga from  $^{80}$ Zn purified by laser ionization, which almost exclusively produces the lower-spin  $3^-$  isomer. We investigate the  $\beta$  decay of  $^{80}$ Ga to  $^{80}$ Ge via  $\gamma$ - $\gamma$  coincidences to try and verify the new 1764(1)-keV  $\gamma$  transition and the proposed levels in  $^{80}$ Ge.

## III. EXPERIMENTAL DETAILS

The data analyzed in this work were obtained in the IS441 experiment performed by the fast-timing collaboration at the ISOLDE facility at CERN, with the aim of investigating neutron-rich nuclei populated in the  $\beta$  decay of Zn isotopes. Results on the structure of <sup>73</sup>Ga, <sup>80</sup>Ga, and <sup>81</sup>Ga have already been published [10,26,27]. This paper reports the investigation of excited states in <sup>80</sup>Ge (N=48, Z=32) populated in the  $\beta$  decay of <sup>80</sup>Ga, which was obtained from the  $\beta^-$  decay of mass-separated selectively ionized <sup>80</sup>Zn source. Out of the two  $\beta$ -decaying 3<sup>-</sup> and 6<sup>-</sup> states in <sup>80</sup>Ga, the <sup>80</sup>Zn  $\beta$  decay populates the 3<sup>-</sup> isomer at 22.4 keV with 98.2(5)% feeding (deduced from the level scheme in [10]) and thus the subsequent <sup>80</sup>Ga  $\beta$  decay proceeds primarily from this state. This is an advantage for the search of feeding to the low-lying 0<sup>+</sup><sub>2</sub> in <sup>80</sup>Ge.

The Zn ions were produced by neutron-induced fission on a heated UC<sub>2</sub>/graphite target. Fast neutrons were produced by the impact of the 1.4-GeV pulsed proton beam from the CERN PS Booster, with an average intensity of 2  $\mu$ A, on a neutron converter. The fission fragments thermally diffused out of the target, traversed a temperature-controlled quartz transfer line that suppressed surface-ionized isobars [28], and reached a W cavity where the ISOLDE Resonance Ionization

Laser Ion Source was used to selectively ionize Zn. A pure and intense  $^{80}$ Zn ion beam was selected in mass using the magnetic high-resolution separator. The mass-separated beam was sent to the experimental area where around 20 000 ions/s were collected in an aluminium catcher foil at the center of the experimental setup. The proton pulses reached the ISOLDE target in multiples of 1.2 s, typically every 2.4 s. After proton impact the released  $^{80}$ Zn ions  $[T_{1/2} = 562(3) \text{ ms}]$  were collected for 600 ms and then diverted by an electrostatic deflector. Data were acquired continuously and sorted using the time of proton impact as reference.

The detection system was composed of two high-purity germanium (HPGe) detectors for high-resolution  $\gamma$  spectroscopy, with relative efficiencies of about 60%, covering an energy range of 30 to 7000 keV. Their energy resolution was 2.0 keV at <sup>60</sup>Co energies. A fast NE111A organic plastic scintillator was used for  $\beta$  particle detection. It was placed less than 0.5 mm away from the aluminium foil to assure high efficiency. Two specially designed LaBr<sub>3</sub>(Ce) crystals [29], coupled to fast photomultiplier tubes, were used for fast-timing measurements. The signals from the detectors were collected by a digital data acquisition system (DAQ) composed of Pixie-4 Digital Gamma Finder cards, designed for fast coincidence  $\gamma$ -ray spectroscopy. Standard sources of <sup>152</sup>Eu and <sup>133</sup>Ba, and online sources of <sup>138</sup>Cs and <sup>140</sup>Ba, were used for the energy and efficiency calibrations of the HPGe detectors. Further details on the experimental procedures are given in [27].

#### IV. RESULTS

The intensities relative to the strongest 659-keV line were extracted using the full-energy peak areas from the  $\gamma$ -ray singles spectrum, illustrated in Fig. 1. The  $^{80}\text{Ga} \rightarrow {}^{80}\text{Ge}$  decay has been optimized by selecting a 1150 to 2250 ms gate after proton impact, and subtracting early (30 to 1140 ms) and delayed (2260 to 3600 ms) spectra in order to reduce the short-lived  $^{80}\text{Zn}$  decay and long-lived  $^{80}\text{Ge}$  and  $^{80}\text{As}$  decay activities, respectively. A  $\beta$  gate is also imposed for better selectivity. This combination results in a virtually background-free spectrum, containing the  $\gamma$  rays attributed to the  $\beta$  decay of the  $^{80}\text{Ga}$  3 $^-$  isomer to  $^{80}\text{Ge}$  in [16] with high statistics.

A weak 1763.8-keV  $\gamma$  line is present in the spectrum (see inset in Fig. 1) with an estimated intensity below 0.2% relative to the 659-keV  $\gamma$  ray. The intensities before and after subtracting the delayed component, and the intensity ratios for different time conditions since proton impact on target, indicate that the 1764-keV peak may contain a contribution from background or long-lived decays such as <sup>80</sup>Ge and <sup>80</sup>As. The strong 1773-keV peak in the spectrum corresponds to a transition in <sup>80</sup>Ge already placed in the level scheme in previous studies [16], whereas the 1742-keV peak arises from the summing of the strongest 1083-keV and 659-keV  $\nu$  rays in the HPGe detectors. To identify the  $\gamma$  transitions that belong to  $^{80}$ Ge, an extensive  $\gamma\gamma$  coincidence study between both HPGe detectors has been performed. A coincidence gate of 267 ns has been used for subtraction of random events. A 1200 to 3600 ms time window after proton impact has been

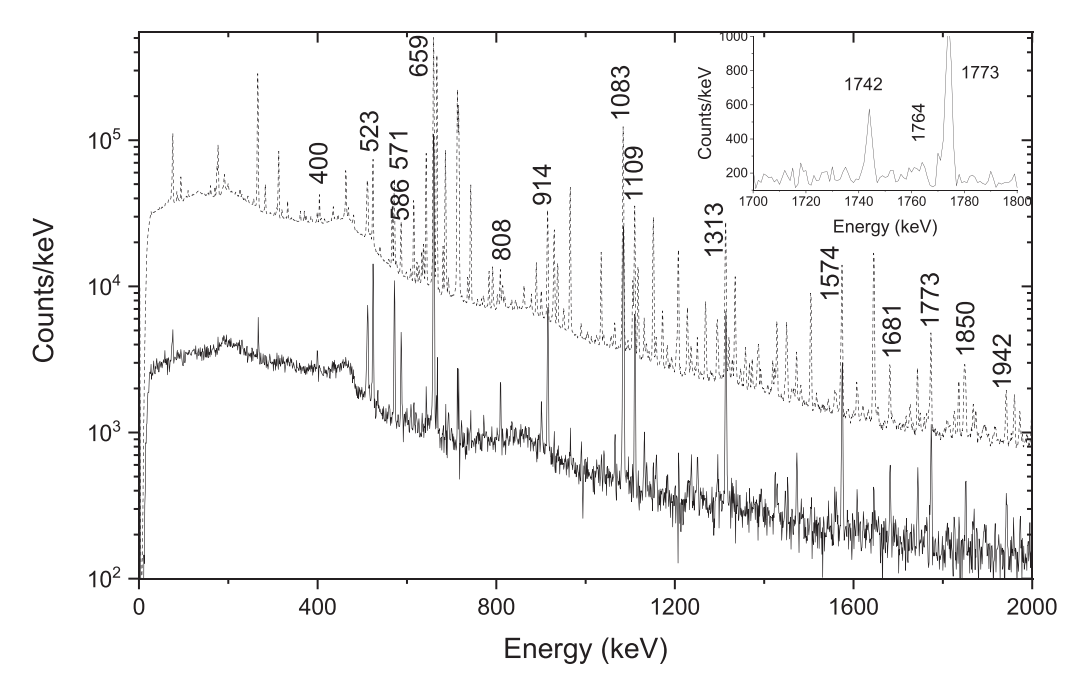


FIG. 1. Dashed line: Beta-gated singles spectrum for the  $\beta$  decay of <sup>80</sup>Ga in the 0-2000 keV energy range. The most intense  $\gamma$  rays in <sup>80</sup>Ge are labeled. Solid line: Beta-gated singles spectrum with subtraction of other isotopes by applying time conditions relative to proton impact on target. The inset shows the region around 1764 keV.

chosen to enhance the  $\beta$  decay of  $^{80}$ Ga to  $^{80}$ Ge. Spectra gated on prominent peaks observed in this study are shown in Fig. 2. Coincidences with the strong 659-keV  $2^+ \rightarrow 0^+$  and 1083-keV  $4^+ \rightarrow 2^+$  transitions are observed. For the latter gate the height of the 659-keV  $2^+ \rightarrow 0^+$  transition reaches almost 1000 counts. In contrast, in the gate on the 1236-keV  $6^+ \rightarrow 4^+$  transition, no counts are observed at 467 keV, the energy of the  $8^+ \rightarrow 6^+$  transition, revealing a weak population of the  $8^+$  3445-keV state. This reflects the small fraction of  $6^{-80}$ Ga parent in the source.

The level scheme obtained in this work is shown in Figs. 3 and 4. A list of energy and intensity values is included in Table I. They are compared to the values reported in [16]. The intensities are unique to this work since most of the  $^{80}$ Ga source is the  $3^-$  isomer. The differences arising from the different parent spin mixture are highlighted in Table I. The forbidden decay from the  $3^-$  isomer can populate  $4^+$  states that can, in turn, decay to the  $6^+$  level at 2978 keV by a single E2 transition. By contrast, the population of the  $8^+$  isomer at 3445 keV would require two sequential E2 transitions that would have to be competitive with higher-energy M1 and E2 transitions to levels at far lower energies.

Owing to the feeding of many of the low-energy levels via this mechanism,  $\beta$  intensities and  $\log ft$  values have only been shown in Figs. 3 and 4 for levels where the intensity is at least equal to or larger than the intensity reported by Hoff *et al.* [16], and also for states that have a  $\gamma$ -ray branch to the  $2^+$  levels. In other words, for levels likely to have spin 2, 3, or 4. Contrary to Hoff *et al.*, who considered a feeding of 18% to the ground state, we chose to neglect any  $\beta$  feeding from the  $3^-$  state in  $^{80}$ Ga to  $0^+$  g.s. in  $^{80}$ Ge and considered a feeding of 0.86(7) via  $\beta$ -delayed neutron emission [30–32].

In [9] the 1764-keV  $\gamma$  ray in <sup>80</sup>Ge was claimed in coincidence with a 639-keV E0 transition. As shown in Figure 2 we observe coincidences of the 1764-keV transition with  $\gamma$  rays at 523, 659, and 1083 keV in <sup>80</sup>Ge, with similar intensities. Reciprocal coincidences with the 523-keV  $4_2^+ \rightarrow 4_1^+$  transition are observed, suggesting its origin from a relatively high spin level. In addition, Fig. 2 shows no coincidence of the 1764-keV  $\gamma$  ray with the 1313-keV transition that deexcites the 1972-keV level.

No transition connecting any of the known levels in Fig. 3 to the  $0^+$  state at 639 keV and the  $2^+$  state at 2403 keV proposed in [9] has been observed either. Specifically we see no connecting transitions from the 2403-keV state to the 659-keV and 1574-keV  $2^+$  levels in our coincidence gates. These data are consistent with the absence of a  $0_2^+$  level at 639 keV.

Hoff et al. [16] proposed a doublet state at 3423 keV (kept by Verney et al. [18]), with the 571-keV transition depopulating a high-spin level, and the transitions at 1158, 1850, and 2764 keV depopulating another level with a suggested lower spin. The relative intensity observed in this study for the 571-keV peak is larger than the previously reported values, indicating that this peak belongs to the decay of the 3<sup>-80</sup>Ga isomer. Hence, only a single level is shown in Fig. 3 at 3423 keV and assigned 3<sup>-</sup> spin and parity, since it should be fed by an allowed  $\beta$  transition. We have additionally checked for the possibility of a doublet of 571-keV  $\gamma$  rays, but it could not be found with our precision. The proposition of a single level at 3423 keV is reinforced by Fig. 5 where the coincidences of new  $\gamma$  rays at 559-, 900-, and 1428-keV are shown. In addition, the 989-keV  $\gamma$  feeds the 3423 keV level according to previous studies [16,24], and we observe it in coincidence

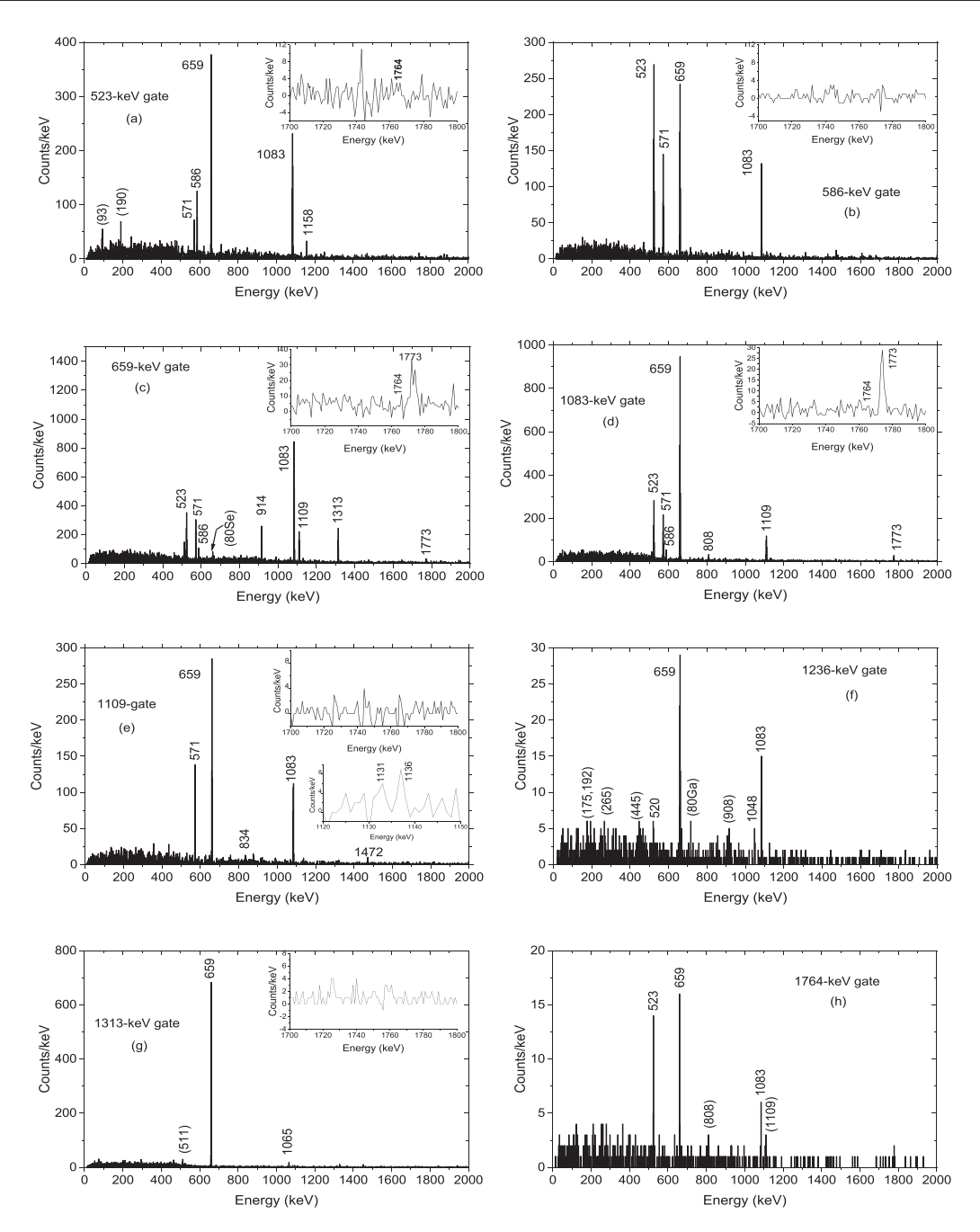


FIG. 2. HPGe  $\gamma$ - $\gamma$  spectra in coincidence with the 523-, 586-, 659-, 1083-, 1109-, 1236-, 1313-, and 1764-keV transitions in <sup>80</sup>Ge. See text for details.

with the deexciting 571-keV transition, as shown in Fig. 5(c) and 5(d).

In previous studies a single 1941-keV  $\gamma$  ray is proposed connecting the levels at 3914 and 1972 keV. Nevertheless, the gated spectra shown in Figs. 5(a) and 5(b) suggest a doublet of transitions of 1942 keV, with the new  $\gamma$  ray connecting the 3515- and 1574-keV levels. The coincidence analysis points to a tentative level at 4030 keV in <sup>80</sup>Ge, with very weak  $\beta$  feeding (log  $ft \approx 7.4$ ), similar to the 8<sup>+</sup> state, that decays to the 2266-keV  $4_2^+$  state. We have checked whether the transition may instead feed the 2852-keV level (see Fig. 3), leading to a state at 4616 keV, but no firm coincidences between

the 1764-keV and the 1109- and 586-keV transitions were found, as illustrated in Fig. 2. We have searched for connecting transitions from the tentative 4030-keV (and 4616-keV) levels to the 659-, 1574-, 1743-, and 1972-keV states without success.

In conclusion, the 1764-keV transition shows coincidences with transitions in  $^{80}\text{Ge}$  and with the E2 659-keV  $\gamma$  ray in particular, contrary to what was observed by Gottardo, where the 1764-keV  $\gamma$  ray was in coincidence with the 639-keV E0 transition. Although the 1764-keV peak might be a doublet, as in the case of  $^{72}\text{Ge}$  [33–35], the  $0_2^+$  at 639 keV cannot be confirmed from our  $\gamma$  spectroscopy data.

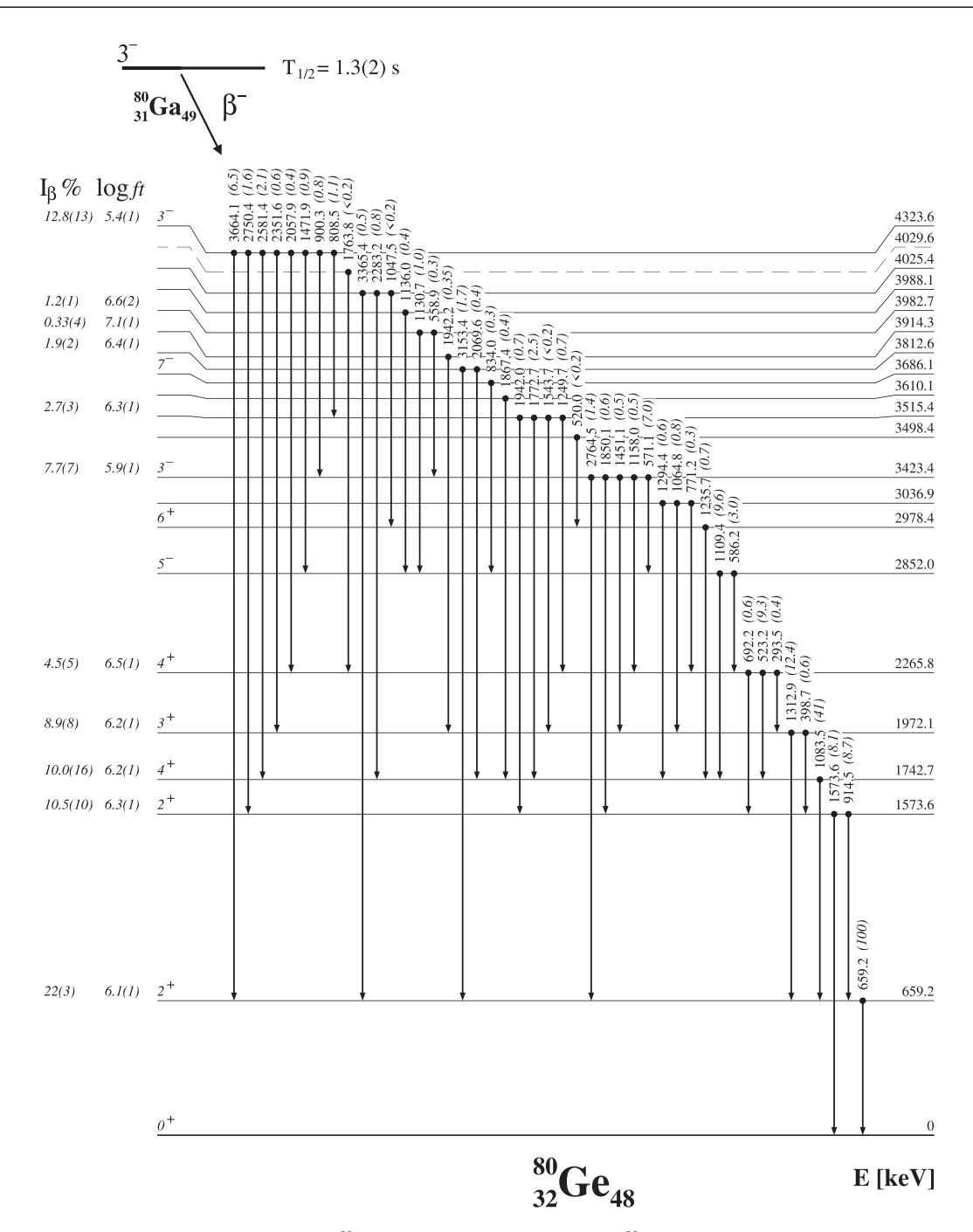


FIG. 3. Low-energy part of the level scheme for  $^{80}$ Ge populated in the  $\beta$  decay of  $^{80}$ Ga obtained in this work, showing the placement of the  $\gamma$  rays in Table I with their associated relative intensities. For absolute intensity per 100 decays, multiply by 0.93(6). Spin-parity values are taken from literature. The log ft values were calculated using  $Q_{\beta}=10312(4)$  keV [36] assuming  $\beta$  decay from the 22.4-keV 3<sup>-</sup> state in  $^{80}$ Ga. The half-life for the 3<sup>-</sup> state is taken from [18]. Firm levels are shown in solid lines, whereas tentative ones are shown in dashed lines.

### V. LEVEL SYSTEMATICS

Neutron rich Ge isotopes up to A=82 have valence protons and neutrons in the same major shell, between the 28 and 50 shell closure, and they have been considered almost spherical. Despite the recent theoretical and experimental studies suggesting shape coexistence, involving deformed and spherical configurations, their nuclear structure has not been completely established yet. Of specific interest is the under-

standing of the anomalous behavior of the  $0_2^+$  state, which goes through a minimum for  $^{72}$ Ge, where it becomes the first excited state [34] below the  $2_1^+$ . Such peculiarity, already observed for  $^{72}$ Kr [37] and  $^{98}$ Mo [38], is not very frequent, and it can be interpreted as a sign of deformation in this region.

The presence of a very low-lying  $0_2^+$  state in  $^{80}$ Ge is not expected from systematics and will entail a modification of our understanding of shape coexistence in the region. Figure 6

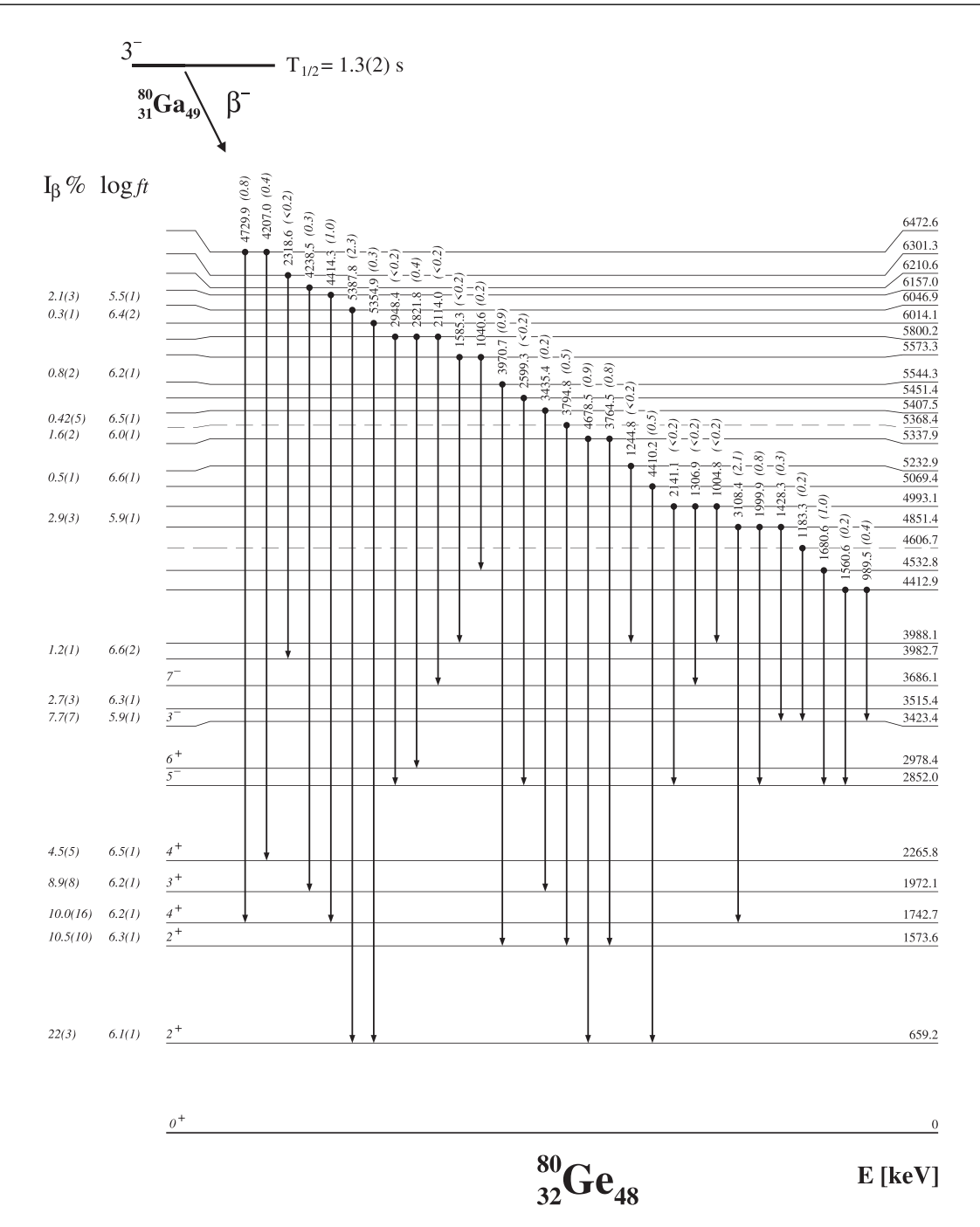


FIG. 4. High-energy part of the level scheme for  $^{80}$ Ge populated in the  $\beta$  decay of  $^{80}$ Ga obtained in this work, showing the placement of the  $\gamma$  rays in Table I with their associated relative intensities.

(top) depicts the systematic trend of the levels in the N=48 even-even isotones from Ni (Z=28) to Mo (Z=42). The yrast states up to  $8^+$  in N=48 isotones can be ascribed to the two-hole  $(vg_{9/2}^{-2})$  configuration in the N=50 closed shell. The subshell closures at Z=38 and Z=40 are apparent with higher  $2^+$  and  $4^+$  states in  $^{86}$ Sr and  $^{88}$ Zr than the corresponding levels in the other isotones. One can notice that gaps between  $8^+$  and  $6^+$  and between  $6^+$  and  $4^+$  for Ge and Se are larger, and that the  $8^+$  state, which does not have a collective origin, is excited at higher energies for  $^{80}$ Ge and

<sup>82</sup>Se. For the  $0_2^+$  states, the deviation between the different isotones is less than 400 keV except for the <sup>88</sup>Zr (N=40) subshell closure, and for <sup>80</sup>Ge where the  $0_2^+$  state proposed in [9] is located below 700 keV. It is worth noting that the gap between the  $0_2^+$  and  $2_2^+$  states is much larger for <sup>80</sup>Ge, more than 900 keV, while it never exceeds 400 keV for the other isotones. The  $0_2^+$  proposed in [9] is therefore not consistent with the N=48 systematics. Similarly to the N=48 isotones, the Z=32 systematics is represented in Fig. 6 (below).

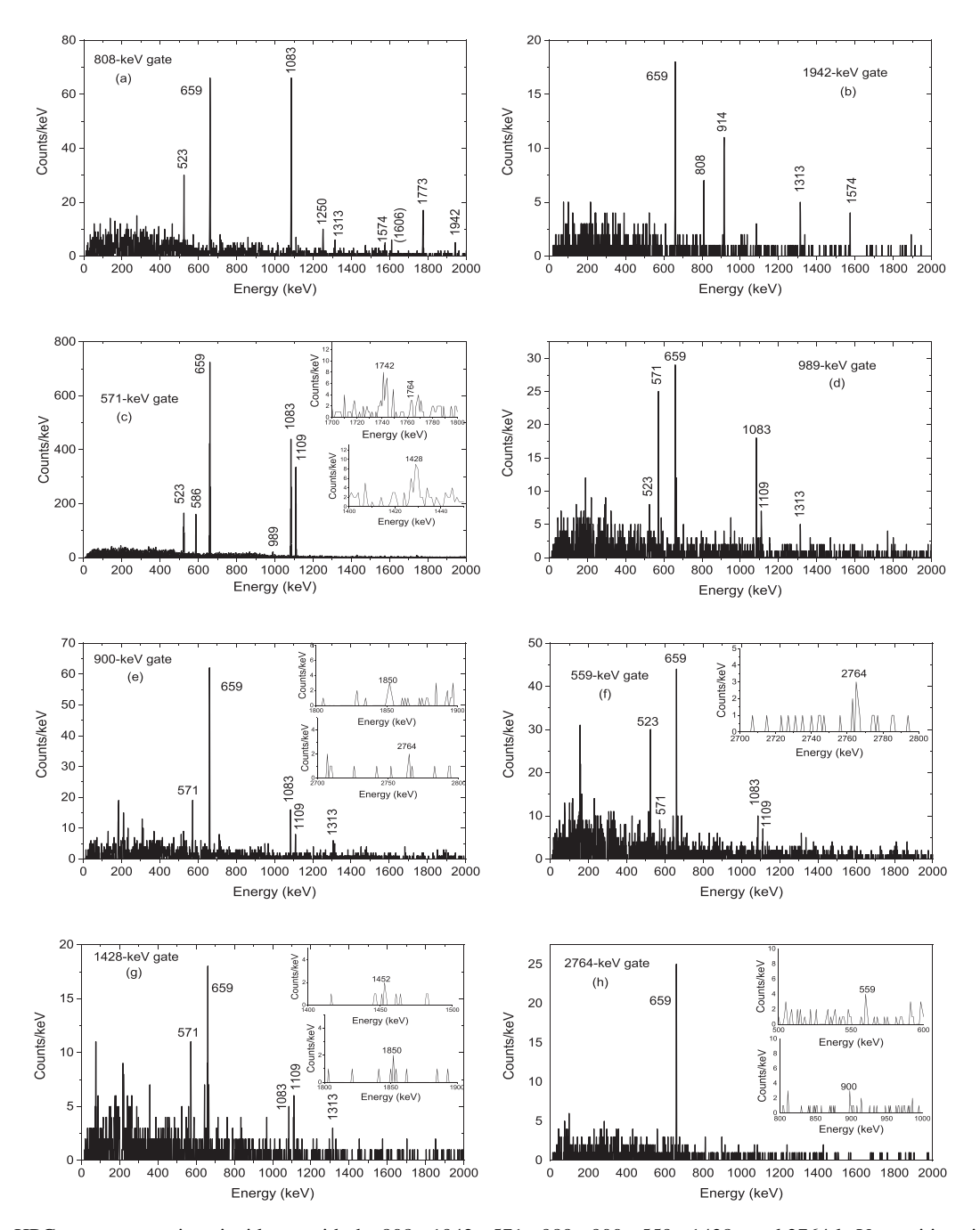


FIG. 5. HPGe  $\gamma$ - $\gamma$  spectra in coincidence with the 808-, 1942-, 571-, 989-, 900-, 559-, 1428-, and 2764-keV transitions in  $^{80}$ Ge.

The excitation energies of the  $2_1^+$ ,  $2_2^+$ , and  $4^+$  states decrease monotonically as the atomic number increases between  $^{70}$ Ge and  $^{76}$ Ge. Thereafter, these energies start to rise. The energy of the  $2_1^+$  state has a local minimum at N=38 rather than in the semiclosed shell at N=40. The gap between the  $2^+$  and  $4^+$  states varies from 681 keV for  $^{82}$ Ge to 1115 keV for  $^{70}$ Ge. The energy ratio  $R_{4/2}=E(4_1^+)/E(2_1^+)$ , one of the observables used to measure the evolution of collectivity, yields  $R_{4/2}=2.64$  for  $^{80}$ Ge. This experimental value suggests that  $^{80}$ Ge is mostly triaxially  $\gamma$  soft, since this ratio is above the value representative of a harmonic vibrator (2.0–2.4) and significantly below that of a rotational nucleus (3.0–3.3).

Unstable shapes in this region do not allow use of a simple version of rotational or vibrational models to explain the spectra; thus, many theoretical studies using different models have been carried out to investigate the structure of Ge isotopes. For example, nuclear density functional theory has been used to analyze the evolution of quadrupole shapes in the  $^{72-82}$ Ge isotopes. Model calculations reproduce the empirical trend of collective observables and predict the evolution of shapes from weakly triaxial in  $^{74}$ Ge to  $\gamma$  soft in  $^{78-80}$ Ge [39].

According to the multiquasiparticle triaxial projected shell model approach, Bhat *et al.* [40] demonstrate that <sup>76</sup>Ge exhibits a rigid  $\gamma$  deformation in its low-lying states, while,

TABLE I.  $\gamma$ -ray transitions in  $^{80}$ Ge, as found in the present work, compared to Hoff's work [16] associated with the level scheme shown in Figs. 3 and 4. The greater value of the intensity between the two works is shown in bold. The transition intensities are normalized to that of the 659-keV  $\gamma$  ray, taken as 100. The tentative  $\gamma$  rays are marked with  $^t$ . The intensities for strong transitions were calculated from the prompt  $\gamma$  singles spectrum and from coincidence spectra for the weaker ones. The errors are based on statistical uncertainties and fitting approximations. The new levels are marked with  $^*$ . Underlined level energies from [16] correspond to the transitions not observed in the present work.

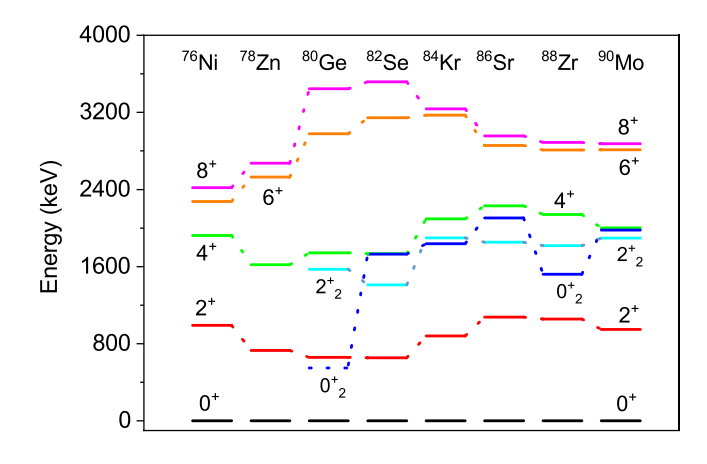
This work		Hoff [16]			
$E_{\gamma}$ (keV)	$I_{\gamma}$	$E_{\gamma}$ (keV)	$I_{\gamma}$	$E_{ m initial}$	$E_{ m final}$
293.5(3)	0.4(3)			2265.8	1972.1
398.7(3)	0.6(1)	399.5(5)	0.5(1)	1972.1	1573.6
		466.76(4)	1.36(5)	3445.1	2978.4
$520.0(3)^t$	< 0.2	519.98(12)	1.25(11)	3498.4	2978.4
523.2(1)	9.3(2)	523.18(4)	12.9(4)	2265.8	1742.7
558.9(8)	0.30(4)			3982.7	3423.4
571.1(1)	7.0(2)	571.06(4)	5.8(2)	3423.4	2852.0
586.2(2)	3.0(2)	586.16(3)	6.6(4)	2852.0	2265.8
659.2(1)	100(2)	659.14(4)	100(3)	659.2	0
692.2(7)	0.6(1)	692.22(5)	0.58(3)	2265.8	1573.6
		707.63(14)	0.3(3)	3686.1	2978.4
771.2(2)	0.30(3)	771.16(5)	0.47(2)	3036.9	2265.8
808.5(5)	1.1(1)	808.45(4)	0.73(4)	4323.6	3515.4
834.0(2)	0.30(4)	834.04(5)	5.6(3)	3686.1	2852.0
900.3(5)	0.8(1)			4323.6	3423.4
914.5(1)	<b>8.7</b> (3)	914.47(5)	5.3(2)	1573.6	659.2
989.5(4)	0.4(1)	989.51(4)	1.13(5)	4412.9	3423.4
$1004.8(5)^t$	< 0.2	1004.79(4)	0.91(4)	4993.1	3988.1
1040.6(3)	0.24(3)	1040.58(4)	1.71(7)	5573.3	4532.8
$1047.5(10)^t$	< 0.2	1047.5(1)	0.3(1)	4025.4	2978.4
1064.8(2)	0.8(1)	1064.80(6)	0.89(5)	3036.9	1972.1
1083.5(1)	41(2)	1083.47(4)	62(2)	1742.7	659.2
1109.4(1)	9.6(4)	1109.36(4)	23.8(8)	2852.0	1742.7
1130.7(1)	1.00(4)	1130.70(6)	1.17(5)	3982.7	2852.0
1136.0(3)	0.4(1)	1135.96(4)	4.2(2)	3988.1	2852.0
		1154.85(9)	0.77(5)	5568.0	4413.2
1158.0(3)	0.5(1)	1158.01(18)	0.34(3)	3423.4	2265.8
1183.3(3)	0.23(3)			*4606.7	3423.4
1235.7(1)	0.7(1)	1235.74(6)	6.2(4)	2978.4	1742.7
1244.8(6) <sup>t</sup>	< 0.2	1244.84(7)	0.79(4)	5232.9	3988.1
1249.7(2)	0.70(4)	1249.76(8)	0.29(3)	3515.4	2265.8
1294.4(3)	0.6(1)	1294.37(8)	0.69(5)	3036.9	1742.7
$1306.9(5)^t$	< 0.2	1306.89(6)	2.26(10)	4993.1	3686.1
1312.9(1)	<b>12.4</b> (7)	1313.00(4)	8.5(3)	1972.1	659.2
1428.3(4)	0.3(1)			4851.4	3423.4
1451.1(2)	0.5(1)			3423.4	1972.1
1471.9(2)	0.9(1)	1471.93(5)	0.67(4)	4323.6	2852.0
$1543.7(5)^t$	< 0.2			3515.4	1972.1
1560.6(5)	0.23(2)	1561	0.3	4412.9	2852.0
1573.6(1)	<b>8.1</b> (7)	1573.57(5)	4.4(2)	1573.6	0.0
$1585.3(4)^t$	< 0.2	1585.34(5)	0.63(3)	5573.3	3988.1
1680.6(1)	1.0(1)	1680.58(5)	<b>5.4</b> (2)	4532.8	2852.0
1763.8(3) <sup>t</sup>	< 0.2			*4029.6	2265.8
1772.7(1)	2.5(2)	1772.67(14)	1.63(12)	3515.4	1742.7
1850.1(3)	0.6(1)	1850.10(5)	0.67(4)	3423.4	1573.6
1867.4(3)	0.40(3)	1867.46(10)	0.31(2)	*3610.1	1742.7

TABLE I. (Continued.)

This work		Hoff [16]			
$E_{\gamma}$ (keV)	$I_{\gamma}$	$E_{\gamma}$ (keV)	$I_{\gamma}$	$E_{ m initial}$	$E_{ m final}$
		1882	0.2	5568.0	3685.89
1942.0(2)	0.7(1)	1941.54(9)	0.59(3)	3515.4	1573.6
1942.2(2)	0.35(4)			3914.3	1972.1
1999.9(1)	0.8(1)	1999.20(10)	0.62(4)	4851.4	2852.0
2057.9(3)	0.40(4)			4323.6	2265.8
2069.6(3)	0.40(3)			*3812.6	1742.7
$2114.0(7)^{t}$	< 0.2	2114.63(7)	1.14(5)	5800.2	3686.1
$2141.1(6)^{t}$	< 0.2	2140.54(13)	0.88(6)	4993.1	2852.0
2283.2(2)	0.8(1)	2283.22(6)	1.28(6)	4025.4	1742.7
$2318.6(3)^t$	< 0.2			*6301.3	3982.7
2351.6(2)	0.6(1)	2351.59(10)	0.39(3)	4323.6	1972.1
2581.4(1)	2.1(2)	2581.35(10)	1.12(5)	4323.6	1742.7
$2599.3(10)^t$	< 0.2	2599.28(16)	0.86(5)	5451.4	2852.0
2750.4(1)	1.6(2)	2750.35(11)	0.64(4)	4323.6	1573.6
2764.5(2)	1.4(1)	2764.45(10)	1.08(6)	3423.4	659.2
2821.8(3)	0.4(1)	2821.82(20)	0.41(4)	5800.2	2978.4
2948.4(6) <sup>t</sup>	< 0.2	2948.40(10)	0.98(5)	5800.2	2852.0
3108.4(1)	2.1(2)	3108.44(10)	1.35(7)	4851.4	1742.7
3153.4(1)	1.7(1)			*3812.6	659.2
3365.4(5)	0.5(1)			4025.4	659.2
3435.4(4)	0.2(1)			*5407.5	1972.1
3664.1(1)	<b>6.5</b> (7)	3664.37(7)	3.7(2)	4323.6	659.2
3764.5(4)	0.8(1)	3764.47(18)	0.48(4)	5337.9	1573.6
3794.8(8)	0.5(1)			*5368.4	1573.6
3970.7(5)	0.9(2)			*5544.3	1573.6
4207.0(3)	0.4(1)			*6472.6	2265.8
4238.5(5)	0.3(1)	4238.6(2)	0.53(4)	*6210.6	1972.1
4410.2(4)	0.5(1)			*5069.4	659.2
4414.3(1)	1.0(1)	4412.6(2)	0.72(5)	6157.0	1742.7
4678.5(1)	0.9(1)	4678.94(20)	0.66(4)	5337.9	659.2
4729.9(4)	0.8(1)	4729.9(3)	0.42(4)	*6472.6	1742.7
5354.9(6)	0.3(1)	5354.9(2)	0.25(2)	*6014.1	659.2
5387.8(1)	2.3(4)	5387.8(2)	1.41(6)	6046.9	659.2

for neighboring nuclei  $^{70,72,74,78,80}$ Ge, configuration mixing of various quasiparticle states can result in a dynamical change for a nucleus from being  $\gamma$ -rigid-like to  $\gamma$ -soft-like. The behavior of the  $0_2^+$  in Ge is rather heterogeneous, with states below 700 keV for  $^{72}$ Ge and  $^{80}$ Ge, around 1200 keV for  $^{70}$ Ge, between 1450 and 1950 keV for  $^{74,76,78}$ Ge and above 2300 keV for  $^{82}$ Ge. In  $^{72}$ Ge the  $0_2^+$  state drops below the  $2^+$  level to become the first excited state, and the same would happen in  $^{80}$ Ge according to [9]. In Ref. [12] by means of large-scale shell-model calculations, the observed variation in excitation of the second  $0_2^+$  state in  $^{70,72,74}$ Ge appears to closely correlate to the  $g_{9/2}$  occupation, induced by a strong proton-neutron interaction.

Thus, the low excitation energy of the  $0_2^+$  in  $^{72}$ Ge is ascribed to the excitation of both protons and neutrons into the  $g_{9/2}$  orbit. We note that the reported  $0_2^+$  in  $^{80}$ Ge is the lowest intruder state in this region, which leads us to speculate about the mechanism that would lower such an intruder state, especially considering that even for  $^{78}$ Ni the intruder state, which is a mixture of 4p4h and 6p6h configurations, lies around



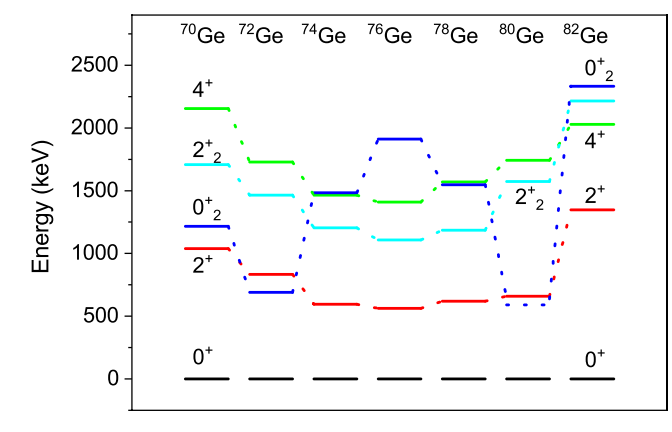


FIG. 6. Level systematics for N=48 isotones (top) and Ge Z=32 isotopes (below). The energy values are taken from the NNDC database [42].

2500 keV [41]. Regarding the systematics of the Z=32 Ge isotopes, the low-lying  $0_2^+$  in  $^{80}$ Ge as proposed earlier [9] is not easy to explain either.

# VI. SHELL-MODEL CALCULATIONS

In order to understand the systematics and the position of the  $0_2^+$  state in  $^{80}$ Ge we have performed shell-model calculations for the energy levels, which we compared to available experimental data. For this purpose, we used ANTOINE [43] and NUSHELLX@MSU [44] codes with the effective interactions JUN45 [45] and ji44bpn [46] respectively. Both JUN45 and jj44b interactions are based on Bonn-C potential with an assumed mass dependence of  $A^{1/3}$ . The JUN45 residual interaction was derived from the best fit to 400 data points for 69 nuclei with  $28 \le N \le 50$  and  $28 \le Z \le 50$ . The singleparticle energies and two-body matrix elements were modified empirically within the  $A \approx 63-96$  mass region. The jj44b Hamiltonian was fitted to 600 binding energies and excitation energies for 77 nuclei with Z = 28-30 and N = 48-50, available in this region. The calculation has been carried out using a <sup>56</sup>Ni closed core and a valence space containing the orbitals  $p_{3/2}$ ,  $f_{5/2}$ ,  $p_{1/2}$ , and  $g_{9/2}$  for protons and neutrons. The results for positive parity states in <sup>80</sup>Ge are depicted in Fig. 7 and compared to the experimental results from the literature. For the sake of completeness, interacting boson model

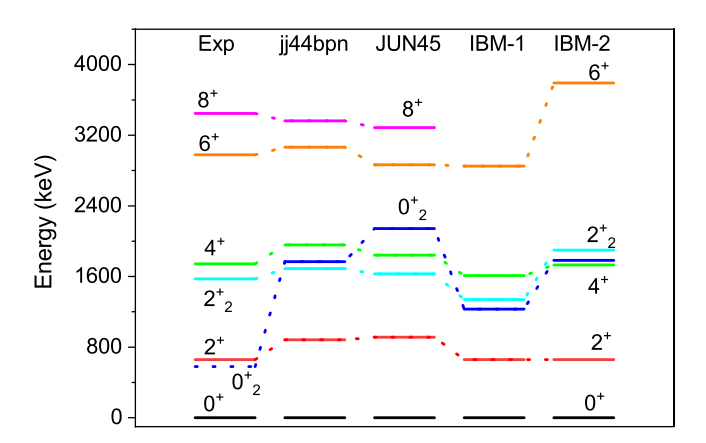


FIG. 7. Comparison of the experimental levels for  $^{80}$ Ge, shell-model calculations with JUN45 and jj44bpn interactions, and IBM calculations from [47]. The model space used for shell-model interactions was  $p_{3/2}f_{5/2}p_{1/2}g_{9/2}$ . Experimental values are from the NNDC database [42].

calculations, without (IBM-1) and with distinction of protons and neutrons (IBM-2), described in [47] are also shown.

The shell-model calculations with both the JUN45 and jj44bpn effective interactions reproduce very well the yrast sequence and the ordering of the excited states (Fig. 7), and yield an excellent description of the  $2^+_2$  state at 1574 keV. As a comparison, the IBM-1 and IBM-2 calculations describe well the first 2<sup>+</sup> and 4<sup>+</sup> states, while the 6<sup>+</sup> state is overestimated by the IBM-2 calculations. Both IBM calculations are not so successful in describing the 2<sup>+</sup><sub>2</sub> state. Concerning the crucial  $0_2^+$  state, the shell-model calculations predict a position well above 1000 keV, with the highest energy being 2140 keV calculated using the JUN45 interaction. The lowest value of 1230 keV is reported in [47] for IBM-1 calculations. In any case none of the available calculations is able to reproduce a very low-lying  $0_2^+$  level in the available model space. Shell-model calculations with both interactions produce such a state above the  $2^+_2$  level.

The calculations have been extended to other even Ge isotopes to investigate the position of the  $0^+_2$  state. The results are represented in Fig. 8 (top panel) and compared to the experimental values and to the IBM calculations [47]. The latter present irregularities in the prediction of the  $0_2^+$  states and fail to reproduce the low intruder state of <sup>72</sup>Ge measured at 691 keV. In contrast the shell-model calculations give an overall good description of the position of the  $0^+_2$  states, the JUN45 interaction reproducing the energies better than the jj44bpn one. The low-lying intruder state of <sup>72</sup>Ge is very well predicted by JUN45 with a deviation around 80 keV, which gives a good indication of the predictive power of this interaction in the region. The absolute deviation of the predictions for the position of the  $0^+_2$  state for both JUN45 and jj44bpn is evident for <sup>80</sup>Ge, larger than 1 MeV, while for other isotopes it is much smaller.

Calculations have also been performed for the  $0_2^+$  states in the N=48 isotones from A=80 to A=90, shown in Fig. 8 (bottom panel). While the calculations successfully reproduce the position of the  $0_2^+$  states well within 400 keV, the

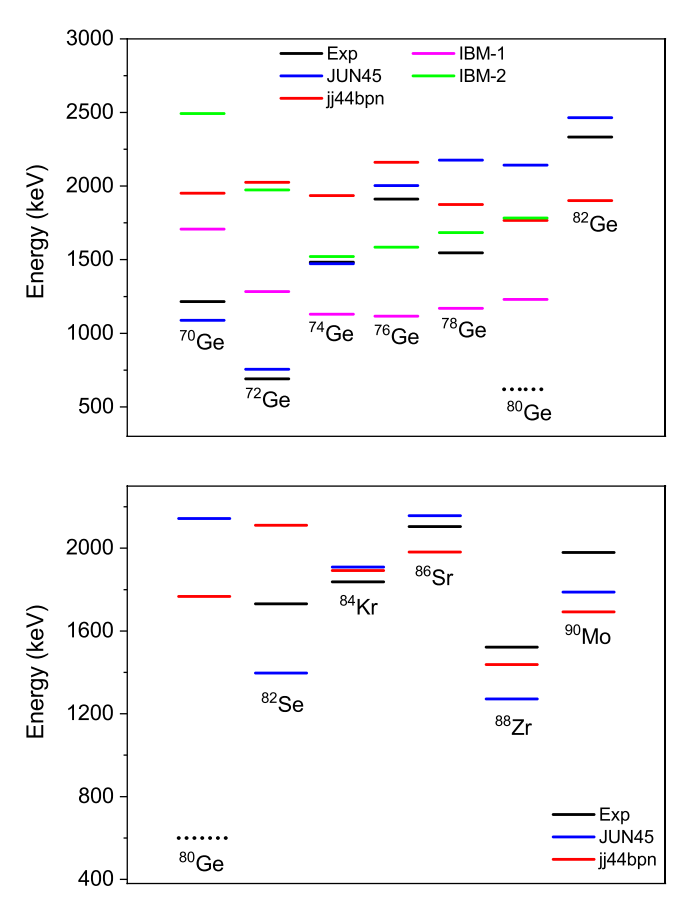


FIG. 8. Comparison of the experimental and calculated values of the  $0_2^+$  state using JUN45, jj44bpn, and IBM interactions for Z=32 isotopes (top) and N=48 isotones (bottom).

calculated  $0_2^+$  energy for  $^{80}$ Ge is 1100 keV apart, as already discussed. We conclude that our calculations in a restricted model space lead to a reasonable description of excitation energies for  $^{80}$ Ge and its neighboring isotopes and isotones, but fail to reproduce a very low-lying  $0_2^+$  state in  $^{80}$ Ge.

#### VII. SUMMARY AND CONCLUSIONS

In this work we have investigated the structure of the N = 48, Z = 32 nucleus <sup>80</sup>Ge at the ISOLDE facility at CERN.

We take advantage of the population of  $^{80}$ Ge in the  $\beta$  decay chain of pure, laser-ionized <sup>80</sup>Zn, whose 0<sup>+</sup> ground state mostly populates the <sup>80</sup>Ga 3<sup>-</sup> 22.4-keV isomer, which then  $\beta$  decays to <sup>80</sup>Ge. The  $0_2^+$  deformed state was suggested at 639(1) keV in a previous study [9] based on the observation of a monopole transition in coincidence with a previously unobserved 1764(1)  $\gamma$  ray. We have examined the position of the intruder  $0_2^+$  state in the nucleus  $^{80}$ Ge in the vicinity of one of the most neutron-rich doubly-magic nuclei, <sup>78</sup>Ni, using  $\gamma$  spectroscopy and shell-model calculations. We have used  $\gamma \gamma$  coincidences to search for feeding to the newly established states. We observe a 1764-keV  $\gamma$  ray in coincidence with the 659-keV  $2_1^+ \rightarrow 0^+$  g.s., and with other transitions in  $^{80}$ Ge, but not feeding the presumed 639-keV  $0_2^+$ . No connecting transitions from previously known levels [16,24] to the proposed 639-keV  $0_2^+$  and 2403-keV  $2_3^+$  states [9] could be established.

Shell-model calculations using the JUN45 and jj44bpn effective interactions in the  $pf_{5/2}g_{9/2}$  model space for both protons and neutrons have been performed to address the location of the deformed  $0_2^+$  state. The calculations satisfactorily reproduce most of the experimental features of the spectra of Ge isotopes and N=48 isotones, but fail to properly describe the very low-lying  $0_2^+$  state in  $^{80}$ Ge. The experimental evidence and the shell-model calculations cannot be reconciled with the presence of such a state at low excitation. A high-statistics  $\gamma$  and electron spectroscopy experiment will be required to completely rule out the existence of the  $0_2^+$  state in  $^{80}$ Ge and the evidence of shape coexistence in  $^{80}$ Ge. One such experiment has been very recently reported [25] and no evidence was found for the  $0_2^+$  639-keV level in  $^{80}$ Ge.

#### **ACKNOWLEDGMENTS**

This work was supported by Spanish national projects FPA2015-65035-P, RTI2018-098868-B-I00, and PID2019-104390GB-I00, by Grupo de Física Nuclear (GFN) at Universidad Complutense (Spain), by the U.S. DoE Grant No. DE-FG02-94ER40834, and by the German BMBF Grant 05P19PKFNA. The support by the European Union Seventh Framework through ENSAR (Contract No. 262010) and by the ISOLDE Collaboration and technical teams is acknowledged.

<sup>[1]</sup> H. Morinaga, Phys. Rev. 101, 254 (1956).

<sup>[2]</sup> G. E. Brown and A. M. Green, Nucl. Phys. 85, 87 (1966).

<sup>[3]</sup> W. J. Gerace and A. M. Green, Nucl. Phys. A 93, 110 (1967).

<sup>[4]</sup> P. Federman and S. Pittel, Phys. Lett. B 69, 385 (1977).

<sup>[5]</sup> E. K. Warburton, J. A. Becker, and B. A. Brown, Phys. Rev. C 41, 1147 (1990).

<sup>[6]</sup> A. Andreyev, M. Huyse, P. Van Duppen, L. Weissman, D. Ackermann, J. Gerl, F. Hessberger, S. Hofmann, A. Kleinbohl, G. Munzenberg *et al.*, Nature (London) 405, 430 (2000).

<sup>[7]</sup> J. Hakala, S. Rahaman, V.-V. Elomaa, T. Eronen, U. Hager, A. Jokinen, A. Kankainen, I. D. Moore, H. Penttilä, S. Rinta-Antila et al., Phys. Rev. Lett. 101, 052502 (2008).

<sup>[8]</sup> R. Taniuchi, C. Santamaria, P. Doornenbal, A. Obertelli, K. Yoneda, G. Authelet, H. Baba, D. Calvet, F. Château, A. Corsi et al., Nature (London) 569, 53 (2019).

<sup>[9]</sup> A. Gottardo, D. Verney, C. Delafosse, F. Ibrahim, B. Roussière, C. Sotty, S. Roccia, C. Andreoiu, C. Costache, M.-C. Delattre et al., Phys. Rev. Lett. 116, 182501 (2016).

<sup>[10]</sup> R. Lică, N. Mărginean, D. G. Ghiţă, H. Mach, L. M. Fraile, G. S. Simpson, A. Aprahamian, C. Bernards, J. A. Briz, B. Bucher et al., Phys. Rev. C 90, 014320 (2014).

<sup>[11]</sup> A. Makishima, M. Asai, T. Ishii, I. Hossain, M. Ogawa, S. Ichikawa, and M. Ishii, Phys. Rev. C 59, R2331 (1999).

- [12] M. Hasegawa, T. Mizusaki, K. Kaneko, and Y. Sun, Nucl. Phys. A 789, 46 (2007).
- [13] R. B. Piercey, A. V. Ramayya, R. M. Ronningen, J. H. Hamilton, V. Maruhn-Rezwani, R. L. Robinson, and H. J. Kim, Phys. Rev. C 19, 1344 (1979).
- [14] H. T. Fortune, Phys. Rev. C 94, 024318 (2016).
- [15] A. Ayangeakaa, R. Janssens, C. Wu, J. Allmond, J. Wood, S. Zhu, M. Albers, S. Almaraz-Calderon, B. Bucher, M. Carpenter et al., Phys. Lett. B 754, 254 (2016).
- [16] P. Hoff and B. Fogelberg, Nucl. Phys. A 368, 210 (1981).
- [17] B. Cheal, E. Mané, J. Billowes, M. L. Bissell, K. Blaum, B. A. Brown, F. C. Charlwood, K. T. Flanagan, D. H. Forest, C. Geppert *et al.*, Phys. Rev. Lett. **104**, 252502 (2010).
- [18] D. Verney, B. Tastet, K. Kolos, F. Le Blanc, F. Ibrahim, M. Cheikh Mhamed, E. Cottereau, P. V. Cuong, F. Didierjean, G. Duchêne *et al.*, Phys. Rev. C **87**, 054307 (2013).
- [19] B. Tastet, Structure des noyaux de gallium, de germanium et d'arsenic riches en neutrons autour de N = 50 et Développement d'une source d'ionisation laser à ALTO, Ph.D. thesis, Université Paris Sud Paris XI, 2011.
- [20] E. Padilla-Rodal, A. Galindo-Uribarri, C. Baktash, J. C. Batchelder, J. R. Beene, R. Bijker, B. A. Brown, O. Castaños, B. Fuentes, J. G. del Campo *et al.*, Phys. Rev. Lett. **94**, 122501 (2005).
- [21] Z. Podolyak, S. Mohammadi, G. de Angelis, Y. H. Zhang, M. Axiotis, D. Bazzaco, P. G. Bizzeti, F. Brandolini, R. Broda, D. Bucurescu *et al.*, Int. J. Mod. Phys. E 13, 123 (2004).
- [22] H. Mach, P. M. Walker, R. Julin, M. Leino, S. Juutinen, M. Stanoiu, Z. Podolyak, R. Wood, A. M. Bruce, T. Bäck et al., J. Phys. G: Nucl. Part. Phys. 31, S1421 (2005).
- [23] T. Faul, Etude de la structure des noyaux riches en neutrons autour du noyau doublement magique <sup>78</sup>Ni, Ph.D. thesis, Université Louis Pasteur - Strasbourg I, 2007.
- [24] A. M. Forney, Nuclear structure studies of <sup>78,80</sup>Ge and adjacent nuclei, Ph.D. thesis, University of Maryland, College Park, 2018
- [25] F. H. Garcia, C. Andreoiu, G. C. Ball, A. Bell, A. B. Garnsworthy, F. Nowacki, C. M. Petrache, A. Poves, K. Whitmore, F. A. Ali et al., Phys. Rev. Lett. 125, 172501 (2020).
- [26] V. Vedia, V. Paziy, L. M. Fraile, H. Mach, W. Walters, A. Aprahamian, C. Bernards, J. A. Briz, B. Bucher, C. J. Chiara, Z. Dlouhy, I. Gheorghe, D. Ghita, P. Hoff, J. Jolie, U. Koster, W. Kurcewicz, R. Lica, N. Marginean, R. Marginean, B. Olaizola,

- J. M. Regis, M. Rudigier, T. Sava, G. S. Simpson, M. Stanoiu, and L. Stroe, Phys. Rev. C **96**, 034311 (2017).
- [27] V. Paziy, L. M. Fraile, H. Mach, B. Olaizola, G. S. Simpson, A. Aprahamian, C. Bernards, J. A. Briz, B. Bucher, C. J. Chiara *et al.*, Phys. Rev. C **102**, 014329 (2020).
- [28] E. Bouquerel, R. Catherall, M. Eller, J. Lettry, S. Marzari, and T. Stora, Eur. Phys. J. Spec. Top. 150, 277 (2007).
- [29] V. Vedia, M. Carmona-Gallardo, L. M. Fraile, H. Mach, and J. M. Udías, Nucl. Instrum Methods Phys. Res., Sect. A 857, 98 (2017).
- [30] G. Rudstam, K. Aleklett, and L. Sihver, At. Data Nucl. Data Tables 53, 1 (1993).
- [31] E. Lund, P. Hoff, K. Aleklett, O. Glomset, and G. Rudstam, Z. Phys. A 294, 233 (1980).
- [32] R. A. Warner and P. L. Reeder, Radiat. Eff. 94, 27 (1986).
- [33] D. C. Camp, Nucl. Phys. A 121, 561 (1968).
- [34] A. Rester, A. Ramayya, J. Hamilton, D. Krmpotic, and P. Rao, Nucl. Phys. A 162, 461 (1971).
- [35] J. Medeiros, C. Zamboni, A. Lapolli, G. Kenchian, and M. Cruz, Appl. Radiat. Isot. 54, 245 (2001).
- [36] M. Wang, W. Huang, F. Kondev, G. Audi, and S. Naimi, Chin. Phys. C 45, 030003 (2021).
- [37] B. Varley, M. Campbell, A. Chishti, W. Gelletly, L. Goettig, C. Lister, A. James, and O. Skeppstedt, Phys. Lett. B 194, 463 (1987).
- [38] M. Zielińska, T. Czosnyka, J. Choiński, J. Iwanicki, P. Napiorkowski, J. Srebrny, Y. Toh, M. Oshima, A. Osa, Y. Utsuno et al., Nucl. Phys. A 712, 3 (2002).
- [39] T. Nikšić, P. Marević, and D. Vretenar, Phys. Rev. C 89, 044325 (2014).
- [40] G. H. Bhat, W. A. Dar, J. A. Sheikh, and Y. Sun, Phys. Rev. C 89, 014328 (2014).
- [41] F. Nowacki, A. Poves, E. Caurier, and B. Bounthong, Phys. Rev. Lett. 117, 272501 (2016).
- [42] National Nuclear Data Center (NNDC), http://www.nndc.bnl. gov/ensdf.
- [43] E. Caurier, G. Martínez-Pinedo, F. Nowack, A. Poves, and A. P. Zuker, Rev. Mod. Phys. 77, 427 (2005).
- [44] B. Brown and W. Rae, Nucl. Data Sheets 120, 115 (2014).
- [45] M. Honma, T. Otsuka, T. Mizusaki, and M. Hjorth-Jensen, Phys. Rev. C **80**, 064323 (2009).
- [46] B. Brown and A. Lisetskiy (unpublished).
- [47] A. R. H. Subber, Turk. J. Phys. 35, 43 (2011).